Original article

Left Ventricular Longitudinal Linear Displacement Versus Global Longitudinal Strain on Cardiovascular Magnetic Resonance

Deslocamento Linear Longitudinal do Ventrículo Esquerdo Comparado ao Strain Longitudinal Global por Ressonância Magnética Cardiovascular

Rafael Almeida Fonseca[1], Sergio Marrone Ribeiro[2], Clerio Francisco de Azevedo Filho[3], Roney Sampaio[1], Flávio Tarasoutchi[1], Carlos Eduardo Rochitte[1]

[1]Heart Institute (InCor), Hospital das Clínicas, School of Medicine, University of São Paulo, São Paulo, SP, Brazil. [2]Botucatu School of Medicine, Paulista State University, UNESP, Botucatu, SP, Brazil. [3]Department of Cardiology, Duke University Medical Center, Durham, NC, USA.

Abstract

Background: Left ventricular (LV) systolic diastolic function is prognostic in cardiovascular diseases and can be assessed via global longitudinal strain (GLS) on echocardiography and cardiac magnetic resonance (CMR). However, GLS by CMR requires the use of expensive software. Longitudinal linear displacement (LLD) may be a simple and inexpensive alternative to GLS, but the two have not been systematically compared.

Objective: To compare LLD with GLS and LV ejection fraction (LVEF) in aortic valve disease patients and controls.

Methods: We included 44 participants (26 with aortic valve disease, 19 controls). GLS was determined using CVI42 software (Circle Cardiovascular Imaging), while the LLD linear measurements of the distance between the base/apex of the LV included maximum displacement (MD), maximum velocity in early diastole (MVED), atrioventricular junction velocity in diastasis (VDS), and VDS/MVED ratio.

Results: DM and MVED were correlated with GLS (r=0.69 and r=0.65, respectively) and LVEF (r=0.47 and r=0.57, p<0.001 for both). DM and MVED showed areas under the receiver operating characteristic curve (AUC) of 0.88 and 0.91, and at the best cut-off point (-0.13 and 0.66), sensitivities of 72.43% and 57.14% and specificities of 80.65% and 87.10%, respectively, compared to GLS. Using LVEF as a reference, we obtained AUC of 0.70 and 0.82, and at the best cut-off point (-0.11 and 0.61), sensitivities of 75.00% and 50.00% and specificities of 72.97% and 78.38%, respectively.

Conclusion: LLD demonstrated similar performance to that of GLS. MD derived from LLD was the best parameter during systole, while MVED was the best during diastole. Our findings demonstrate the routine, quick, and inexpensive assessment of diastolic function on CMR.

Keywords: Magnetic Resonance; Myocardial Contraction; Aortic Valve Stenosis; Aortic Valve Insufficiency; Diastole.

Resumo

Introdução: A função sistodiastólica do ventrículo esquerdo é prognóstica nas doenças cardiovasculares e pode ser avaliada por *strain* longitudinal global por meio de ecocardiografia e de ressonância magnética cardíaca. O *strain longitudinal global* pela ressonância magnética cardíaca exige a utilização de *software* de alto custo. O deslocamento linear longitudinal do ventrículo esquerdo pode ser uma alternativa simples e barata ao *strain* longitudinal global, porém eles não foram ainda comparados sistematicamente.

Objetivo: Comparar o deslocamento linear longitudinal com o *strain* longitudinal global e fração de ejeção do ventrículo esquerdo em valvopatas aórticos e controles.

Métodos: Incluímos 44 participantes (26 valvopatas aórticos/19 controles). O *strain* longitudinal global utilizou *software* específico (*Circle Cardiovascular Imaging* 42) e o deslocamento linear longitudinal apenas medidas lineares de distância entre a base e o ápex do ventrículo esquerdo, gerando deslocamento máximo, velocidade máxima no início da diástole, velocidade na diástase e a relação entre velocidade na diástase e velocidade máxima no início da diástole.

Resultados: Deslocamento máximo e velocidade máxima no início da diástole correlacionaram-se com *strain* longitudinal global (r=0,69 e r=0,65 respectivamente) e com a fração de ejeção do ventrículo esquerdo (r=0,47 e r=0,57, p<0,001 para ambos). Deslocamento

Mailing Address: Carlos Eduardo Rochitte •
Instituto do Coração, Faculdade de Medicina, Universidade de São Paulo, Avenida Dr. Enéas de Carvalho Aguiar, 44, Andar AB, Cerqueira César.
CEP: 05403-000 – São Paulo, SP, Brazil.
E-mail: rochitte@incor.usp.br
Manuscript received 5/11/2022; revised 5/18/2022; accepted 5/25/2022

DOI: 10.47593/2675-312X/20223502eabc304

máximo e velocidade máxima no início da diástole apresentaram área sob a curva Característica de Operação do Receptor de 0,88 e 0,91 e, no melhor ponto de corte (-0,13 e 0,66), sensibilidade de 72,43% e 57,14% e especificidade 80,65% e 87,10%, respectivamente, quando comparados ao *strain* longitudinal global. Utilizando a fração de ejeção do ventrículo esquerdo como referência, foram obtidos 0,70 e 0,82, e, no melhor ponto de corte (-0,11 e 0,61), sensibilidade de 75,00% e 50,00% e especificidade 72,97% e 78,38%, respectivamente.

Conclusão: O deslocamento linear longitudinal foi semelhante ao *strain* longitudinal global. O deslocamento máximo derivado do deslocamento linear longitudinal foi o melhor parâmetro na sístole, enquanto a velocidade máxima no início da diástole foi o melhor na diástole, o que possibilita a avaliação da função diastólica pela ressonância magnética cardíaca na rotina clínica de forma rápida e sem custo adicional.

Palavras-chave: Ressonância Magnética; Contração Miocárdica; Estenose da Valva Aórtica; Insuficiência da Valva Aórtica; Diástole.

Introduction

Systolic and diastolic dysfunction are important markers of several cardiovascular diseases in clinical practice.[1] Studies evaluating myocardial strain demonstrated high ability for the early detection of contractile dysfunction in several cardiovascular diseases.[2] The myocardial strain technique is based on myocardial architecture analysis and evaluates three distinct layers: subendocardial, formed by longitudinal fibers oriented from the base to the apex; middle of the wall, with circumferential fibers; and subepicardial, with longitudinal fibers oriented from the apex to the base.[2]

The strain is often measured by two modalities, speckle tracking by echocardiography (ECHO) and feature tracking imaging (FTI) by cardiac magnetic resonance imaging (CMRI).[3,4] ECHO, which analyzes small groups of pixels in the myocardium created by the interaction of ultrasonic beams and the heart muscle with specific grayscale characteristics, is the most widely used modality in clinical practice. CMRI can assess GLS via two techniques. The first technique is myocardial tissue tagging, which identifies simple linear or grid patterns applied to the CMRI image during its acquisition and is considered the gold standard for assessing GLS against which ECHO was validated.[5] However, this technique requires the acquisition of specific tagging images, demanding additional time for CMRI study.

The new FTI technique was recently developed for GLS assessments using conventional cine-MRI. This technique uses principles similar to speckle-tracking used in ECHO but that are applied to CMRI to track specific pixels characteristics throughout the cardiac cycle.[6] Studies of patients developing diastolic dysfunction in pathologies such as aortic stenosis (AoS) and aortic insufficiency (AoI) demonstrated a left ventricular (LV) ejection fraction (LVEF) within the normal range and changed strain, indicating the presence of a diastolic dysfunction component in addition to the incipient contractile dysfunction not detected by LVEF. These data indicate that GLS, which incorporates systolic and diastolic function, is more sensitive than LVEF for assessing ventricular contraction mechanics.[7,8]

GLS is not usually assessed by FTI CMRI in clinical routine, as it requires additional post-processing time and specialized and expensive software. This technique requires the acquisition of endocardial and epicardial contours for all cardiac phases on a cine-MRI scan. Our group evaluated a new technique that is simple to apply, requires no specialized software, and can be performed using simple and free image viewer software. This technique is based on LV longitudinal linear displacement (LLD), more specifically on the linear basal-apical shortening of the LV. In this previous study, longitudinal shortening detected systolic and diastolic function changes in patients with aortic valve disease (AVD) versus normal controls.

Although LLD was already compared with diastolic dysfunction by ECHO[9] and in specific groups of patients with proven diastolic dysfunction,[10] it has not yet been compared with GLS by FTI CMRI. Thus, this study aimed to compare LLD and GLS measured by the FTI technique.

Methods

Study population

This study included 26 patients with severe AVD eligible for aortic valve replacement surgery with LVEF within the normal range who underwent CMRI as part of their clinical evaluation. It also included 19 healthy controls. Of the patients with AVD, 11 (42.3%) had aortic regurgitation and 15 (57.7%) had AoS. The exclusion criteria were age below 18 and above 85 years, diabetes mellitus, systemic arterial hypertension, dyslipidemia, or significant concomitant coronary disease. All patients aged over 40 years underwent coronary angiography, and those with significant coronary artery disease (luminal stenosis > 50%) were excluded. Patients with concomitant mitral valve disease, previous cardiac surgery, or contraindications to CMRI; who were using pacemakers, metal clips, or other ferromagnetic structures; or who had claustrophobia were also excluded.

Baseline GLS and LLD were established in 19 healthy volunteers with no significant medical history. Patients underwent CMRI with a 1.5 Tesla clinical magnet (Signa CV/i; GE Medical Systems, Waukesha, WI, USA) and dedicated cardiac coil. After the heart was located, 8–12 contiguous short-axis slices covering the entire LV (8-mm slice thickness and 2-mm inter-slice interval) and long-axis slices (two- and four-chamber planes and LV outflow tract) were prescribed. Cine-MRI scans were acquired with a steady-state free precession pulse sequence with high temporal resolution (<50 ms between phases) and with other conventional parameters: TR, 3.9 ms; TE, 1.8 ms; flip angle, 45°; receiver bandwidth, ±125 kHz; field of view, 34 × 34 cm; 256 × 160 matrix; and voxel size, 1.3 × 2.1 × 8.0 mm.

Image analysis using feature tracking imaging technique to obtain GLS

Global longitudinal strain was analyzed using cine-MRI images in four-chamber long-axis view and along 20 cardiac phases. CVI42 software (Circle Cardiovascular Imaging, Calgary, Canada) and the Tissue Tracking tool were used to identify the diastolic phase, with manual definition of the endocardial and

epicardial contours, which are automatically propagated by the software to the other cardiac phases. Subsequently, myocardial GLS was automatically calculated by the software using a Eulerian mathematical principle that represents a measure of ventricular strain (Figure 1).[11] GLS numerical data were stored in the software and exported to data sheets for further analysis.

Image analysis using the longitudinal linear displacement (LLD) technique

As in GLS analysis, LLD was performed on cine-MRI images in four-chamber long-axis view. The basal atrioventricular junction (AVJ) position was defined in end-diastole and its longitudinal displacement was measured in relation to a reference line drawn between the LV apex (epicardium contour, low-intensity line corresponding to the myocardial and epicardial fat interface) and the lower limit (low-intensity line) of the coronary sinus running along the atrioventricular groove immediately lateral to the AVJ. A simple straight line was traced through the cardiac cycle along all phases between the basal and apical landmarks using a DICOM Webpax visualization platform (Heart Imaging Technologies, LLC, Durham, NC, USA) (Figure 2). Phase-by-phase LV longitudinal measurements were subsequently divided by the longitudinal length at end-diastole (maximum length) to provide percentage AVJ displacement values during the 20 phases.

$$\text{(AVJ dis.\%).}\ AVJ\ dis.(\%) = \frac{LM(phase)}{CM}$$

Longitudinal displacement (D) versus time was analyzed by subtracting the maximum percentage AVJ displacement (max AVJ des. %) by the minimum for each phase (min. phase) divided by the max AVJ des. % as shown in the equation below.

$$D = \frac{AVJ\ dis.(\%)Max - Min(phase)}{Max\ AVJ\ dis.(\%)}$$

LLD parameters were extracted from the generated longitudinal displacement (D) versus time graph: maximum displacement (MD), maximum velocity in early diastole (MVED), best-fit line of normalized AVJ velocity in diastasis (VDS), and VDS/MVED ratio. MD was extracted through the minimum over the data range obtained from D as shown in the equation below.

$$MD = Minimum\ D\ (phase\ by\ phase)$$

The MVED of each participant was acquired through a regression slope on the displacement versus time graph adjusted for early diastole (Figure 2). The same method was used for VDS considering the time of diastasis.

Statistical analysis

Sample size was related to the number of patients with a confirmed diagnosis available for analysis (convenience sample), which corroborates the literature in the area.[10,12] Normality was assessed by the Shapiro-Wilk test. Simple linear regression analyses were performed for each of the LLD parameters (MVED, VDS, MD, and VDS/MVED) with GLS and LVEF. A GLS cutoff point of -13%, which corresponds to the 99th percentile of the values measured in the control group, was used as the limit of normality. A normal LVEF was considered those greater than or equal to 55%. We evaluated the accuracy, sensitivity, and specificity of the LLD parameters (MVED, VDS, MD, and VDS/MVED) using FTI GLS and LVEF with the normality thresholds defined above as the reference method. The receiver operating characteristic (ROC) curves and the cut-point test were used to define the optimal sensitivity and specificity threshold. Stata software version 13 for Macintosh was used for the statistical analysis considering values of $p < 0.05$ as statistically significant.

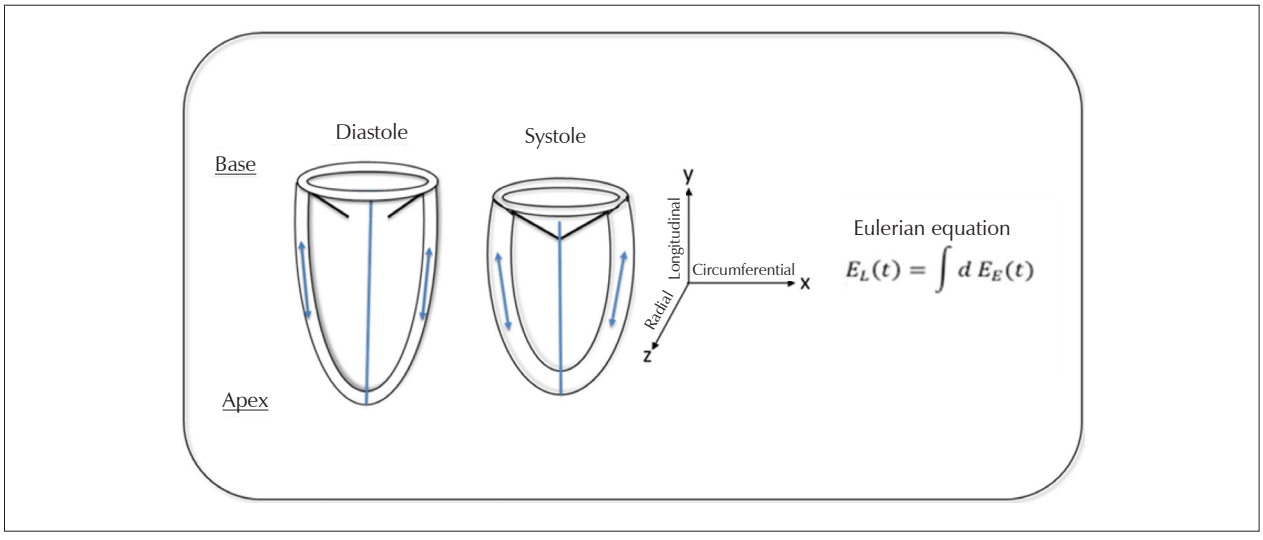

Figure 1 – *Illustration of myocardial deformation by the Eulerian equation used to extract the global longitudinal strain values used in our study using CVI 42 software.*

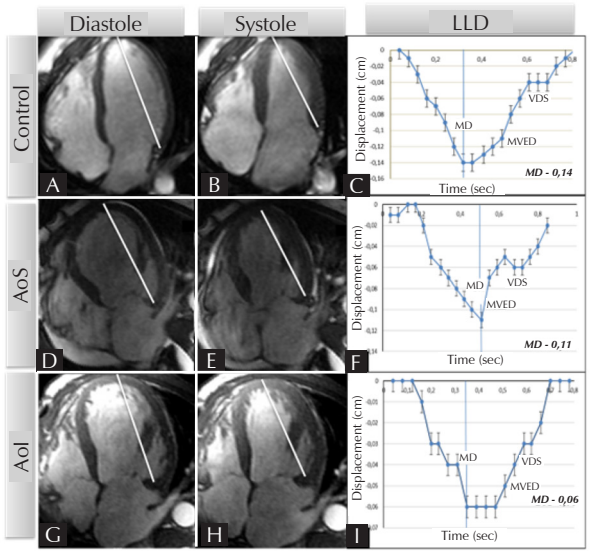

AoI: aortic insufficiency; AoS: aortic stenosis; LLD: longitudinal linear displacement.

Figure 2 – *Panel demonstrating longitudinal linear displacement (LLD) analysis in patients with valve disease and normal controls. (A) and (B) represent the cardiac cycle phase. (C) represents the LLD parameter curve.*

Results

Population characteristics

The group of healthy volunteers included 10 men and nine women with a mean age of 43.1 ± 11.8 years (range, 24–58 years). The patient group included 19 men and seven women with a mean age of 46.8 ± 13.7 years (range, 26–72 years). The participants' clinical characteristics including cardiovascular history, risk factors, and CMRI data are presented in Table 1.

Cardiovascular magnetic resonance imaging

Table 2 shows the results of GLS, morphology, volume, and global LV function measurements for all groups. Figure 3 shows sample GLS analyses in each group and endocardial and epicardial contours.

The MVED, MD, VDS, and VDS/MVED correlation coefficients (r) and (p) are presented in Table 3. MD and MVED showed strong and significant correlations compared with the GLS approach for both the total sample and for only patients with AVD. Compared with LVEF, the correlations were more evident and significant for all participants (Table 3). The linear regression of MD versus GLS showed a positive correlation with an $r = 0.69$ and $p < 0.001$ for the total sample and an $r = 0.66$ and $p < 0.001$ for patients with AVD (Figure 4). Comparison of MD and LVEF resulted in an $r = 0.47$ and $p < 0.001$ (Figure 4).

The linear regression of MVED versus GLS showed a negative correlation of an $r = -0.65$ and $p < 0.001$ for the total sample and an $r = -0.53$ and $p < 0.005$ for patients with AVD (Figure 5). MVED is positively correlated with LVEF and showed an $r = 0.57$ and $p < 0.001$ for all participants.

The evaluation of VDS and VDS/MVED with GLS and LVEF

Table 1 – Patients' clinical characteristics.

Característica	OAI	AoS	Controls	p/p*
Demographics				
Total (N = 45)	11 (42.3)	15 (57.7)	19	
Men	10 (90.9)	9 (60.0)	10 (52.6)	0.079/0.101
Age, years	46.0±15.7	48±11.3	38.1±10.5	0.610/0.039
Weight, kg	76.6±10.6	71.2±11.9	67.9±15.3	0.336/0.356
BMI, kg/m^2	27.9±3.5	26.3±3.8	23.5±3.6	0.382/0.021
BSA, m^2	1.8±3.5	1.7±0.1	1.47±0.2	0.209/0.696
Rheumatic	9 (81.8)	3 (20.0)	-	
Bicuspid	2 (18.2)	8 (53.3)	-	
Degeneration/calcification	0	4 (26.7)	-	
Heart rate, bpm	65.0±11.9	81.5±20.7	70.1±10.6	0.027/0.019
SBP	126.7±11.9	121.5±15.2	111.6±8.9	0.505/0.018
DBP	80±8.9	71.8±12.8	71.3±6.6	0.183/0.143
Risk factors and cardiovascular history				
Angina	0 (0.0)	1 (6.7)	-	0.465
Hypertension	6 (54.6)	1 (6.7)	-	0.465
Syncope	0	6 (40.0)	-	0.100
Diabetes	0	1 (13.3)	-	0.342
Hypercholesterolemia	0	0	-	-
Smoker	0 (0.0)	5 (33.3)	-	0.100
Family history and CAD	4 (34.4)	3 (20.0)		0.190
NYHA classification > I (II and III)	11 (100.0)	15 (100.0)	19 (100.0)	0.526

*Absolute values and percentages in parentheses, n (%). AoI, aortic insufficiency; AoS, aortic stenosis; BMI, body mass index; BSA, body surface area; CAD, coronary artery disease; DBP, diastolic blood pressure; EDV, end-diastolic volume; ESV, end-systolic volume; GLS, global longitudinal strain; LV, left ventricle; LVEF, left ventricular ejection fraction; NYHA, New York Heart Association; SBP, systolic blood pressure. *Comparison between three groups, including controls; remaining p values for comparison between aortic insufficiency and stenosis. The criteria for defining concentric hypertrophy are LV mass/EDV ratio > 1.16 g/mL). Ref: Dweck MR et al. J Cardiovasc Magn Reson 2012.*

showed weak correlations or discrete associations, some of which were not statistically significant for the total sample or patients with AVD (Table 3).

Table 4 shows the diagnostic performance analysis data for MVED, MD, VDS, and VDS/MVED measures to predict GLS and LVEF. MD and MVED again demonstrated better diagnostic performance than LVEF and GLS. The MD versus GLS longitudinal axis presented an area under the ROC curve of 0.88. When the best cutoff point (-0.13) was defined, MD demonstrated 72.43% sensitivity and 86.65% specificity (Figure 6). The analysis with LVEF showed an area of 0.70, sensitivity of 75.00%, and specificity of 72.97% (at the best cutoff point under the ROC curve, -0.11) (Figure 6). MVED versus GLS showed an area of 0.91, sensitivity of 57.14%, and specificity of 87.10% (cutoff point of 0.53). The analysis of MVED and LVEF resulted in an area of 0.82, sensitivity of 50.00%, and specificity of 78.38% (at the best cutoff point of 0.61) (Figure 7). VDS and VDS/MVED demonstrated inferior diagnostic performance (Table 4).

Table 2 – Cardiac magnetic resonance imaging data by study group.

Characteristic	IAo	EAo	Controles	p/p*
GLS	-10.7±2.3	-13.0±3.2	15.9±1.7	<0.001
LVEDV, mL	29.6±68.5	179.99±42.1	129.5±24.7	<0.001
LVESV, mL	148.9±60.4	82.0±28.7	45.5±9.4	<0.001
LVEF, %	51.7±11.4	55.1±9.1	64.7±5.3	<0.001
LV mass, g	264.2±42.4	272.8±45.5	118.1±40.5	<0.001
Eccentric hypertrophy	10 (90.9)	1 (6.7)		
Concentric hypertrophy	1 (9.1)	14 (93.30		
MD	-0.09	0.12	0.16	
MVED	0.47	0.78	1.43	
VDS	0.09	0.31	0.28	
VDS/MVED	0.44	0.23	0.21	

AoI, aortic insufficiency; AoS, aortic stenosis; GLS, global longitudinal strain; LVEDV, left ventricular end-diastolic volume; LVEF, left ventricular ejection fraction; LVESV, left ventricular end-systolic volume; MD, maximum displacement; MVED, maximum velocity in early diastole, VDS, best-fit line of normalized atrioventricular junction velocity in diastasis. All indicates AoI, AoS, and controls.

Discussion

This study demonstrated that the assessment of LV diastolic

Table 3 – Linear regression analysis of MD, MVED, VDS, and VDS/MVED.

All	Strain (%)		LVEF (%)	
MD, cm	0.69	<0.001	0.47	<0.001
MVED, s^{-1}	0.65	<0.001	0.57	<0.001
VDS, s^{-1}	0.01	<0.920	0.09	<0.559
VDS/MVED	0.31	<0.035	0.43	<0.003
Aortic valve disease r,(p)				
MD, cm	0.66	<0.001	0.23	<0.244
MVED, s^{-1}	0.53	<0.005*	0.39	<0.049
VDS, s^{-1}	0.43	<0.027	0.25	<0.215
VDS/MVED	0.04	<0.837	0.18	<0.378

LVEF, left ventricular ejection fraction; MD, maximum displacement; MVED, maximum velocity in early diastole, VDS, best-fit line of normalized atrioventricular junction velocity in diastasis. All indicates AoI, AoS, and controls.

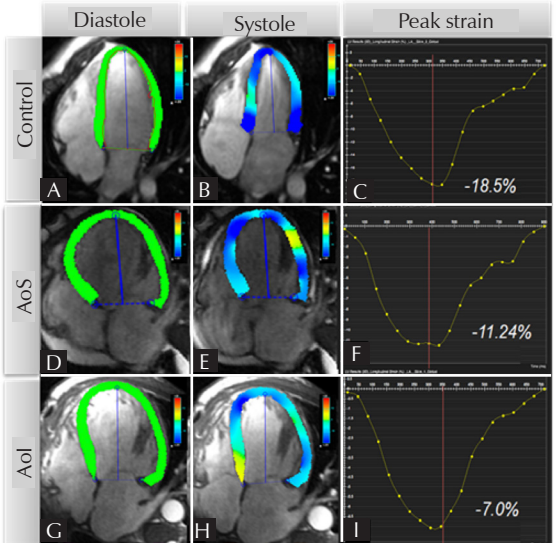

AoI:aortic insufficiency; AoS: aortic stenosis.

Figure 3 – *Panel demonstrating global longitudinal strain analyses detailing endocardial and epicardial contours. Peak strain is shown. (A) and (B) represent the analyses of normal control volunteers with peak stain of 18.5% (C). (D) and (E) show the analyses of patients with aortic stenosis and a strain peak of 7.0% (G). (F) and (H) present the strain of patients with aortic insufficiency and a peak strain of 11.0% (I).*

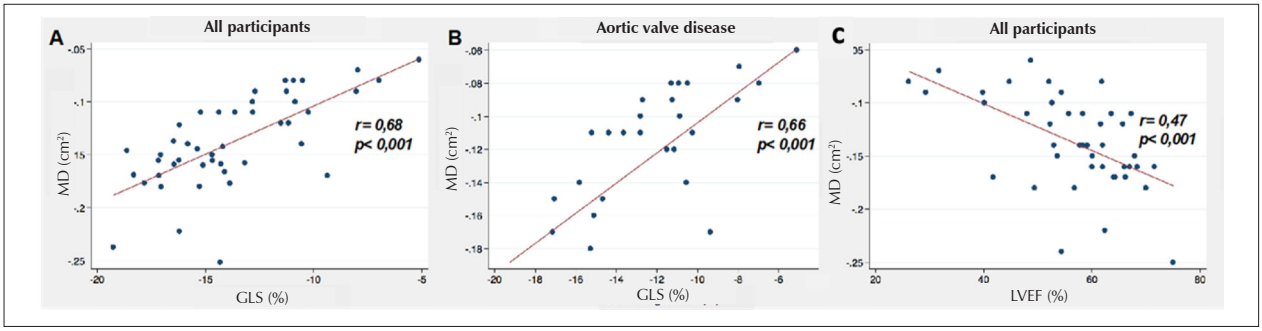

Figure 4 – *(A) and (B) show the correlation between maximum atrioventricular junction displacement and global longitudinal strain. (A) shows the analysis of all patients. (B) shows the regression of patients with aortic valve disease.*

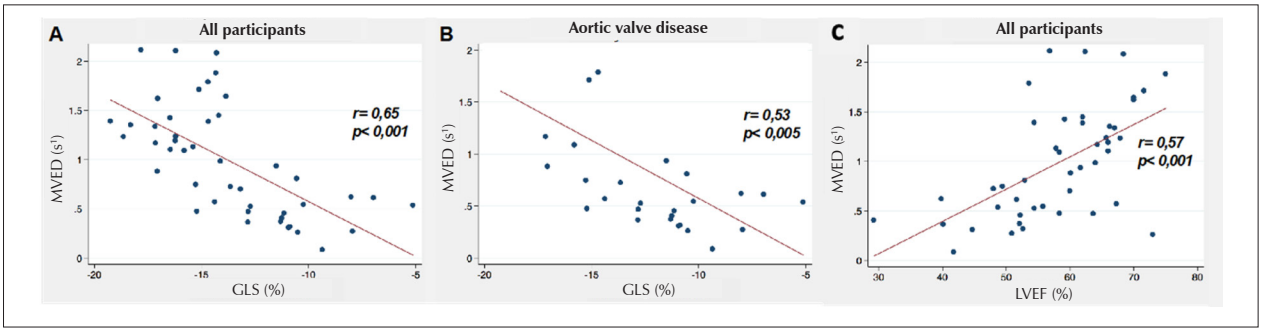

Figure 5 – *(A) and (B) show the correlation between maximum atrioventricular junction displacement and left ventricular ejection fraction. (A) shows the analysis of all patients. (B) shows the regression of patients with aortic valve disease.*

Table 4 – Diagnostic performance of MD, MVED, VDS, and VDS/MVED on the receiver operating characteristic curve.

	AUC	Sensitivity	Specificity	PPV	NPV
Strain, %					
MD, cm	0.88	72.43	80.65	62.50	86.21
MVED, s^{-1}	0.91	57.14	87.10	66.67	81.82
VDS, s^{-1}	0.56	57.14	64.52	42.11	76.92
VDS/MVED	0.68	78.57	58.06	45.83	85.71
LVEF (%)					
MD, cm	0.70	75.00	72.97	37.50	93.10
MVED, s^{-1}	0.82	50.00	78.38	33.33	87.88
VDS, s^{-1}	0.67	62.50	62.16	26.32	88.46
VDS/MVED	0.82	100.00	56.76	33.33	100.00

AUC, area under the receiver operating characteristic curve; LVEF, left ventricular ejection fraction; MD, maximum displacement; MVED, maximum velocity in early diastole; NPV, negative predictive value; PPV, positive predictive value; VDS, best-fit line of normalized atrioventricular junction velocity in diastasis.

dysfunction using linear CMRI parameters (MD and MVED) has statistically high correlation and diagnostic accuracy to that of GLS measured by FTI and LVEF in patients with AoS and AoI as well as in normal controls.

These data corroborate and reinforce the results of the study by Ribeiro et al., in which LV linear measurements (MVED, MD, VDS, and VDS/MVED) differed significantly between patients with AVD and normal controls. In our study, we validated linear measurements derived from LLD versus GLS measured by specific FTI software and LVEF. Saba et al. used a similar technique and obtained slightly higher linear measurements in the normal control group than in that of our study (-0.165).[9] This is probably due to the use of a less lateral anatomical landmark and, therefore, a lower diastolic value of this distance that results in a greater percentage variation with the systolic linear measurement. The most lateral point chosen in the present study increased the precision and reproducibility of its visual definition by the observer. On cine-MRI, coronary sinus interface in the atrioventricular groove is better defined than the junction of the mitral valve leaflets in the mitral fibrous annulus. We used only one AVJ displacement measurement, with a better defined reference point on the AVJ lateral wall instead of two, thus simplifying and making the measurements faster and more practical.

Saba et al. validated linear measurements with peak systolic strain using tissue Doppler to assess diastolic function; however, our study demonstrated a statistically significant correlation between MD and GLS by FTI CMRI. These data reinforce the relevance of MD on CMRI in the assessment of systolic dysfunction. Furthermore, the area under the ROC curve of MD versus GLS showed high accuracy (0.88) for assessing systolic function. MVED demonstrated high accuracy when correlated with GLS (0.91). For the first time, this information allows the use of a method to analyze

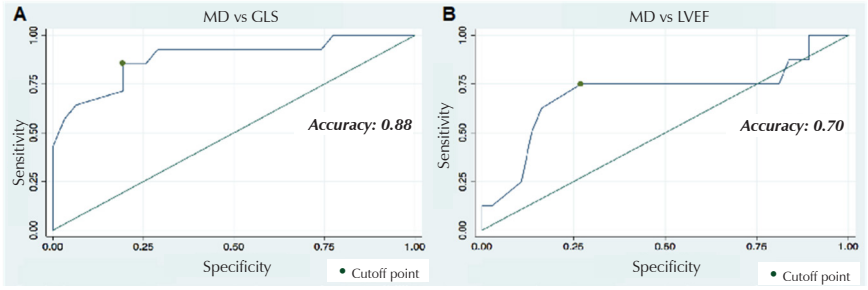

MD: maximum displacement; LVEF: left ventricular ejection fraction.

Figure 6 – *(A) Receiver operating characteristic curve between global longitudinal strain and maximum velocity in early diastole indicating the best cutoff point. (B) Atrioventricular junction velocity in diastasis and left ventricular ejection fraction performance.*

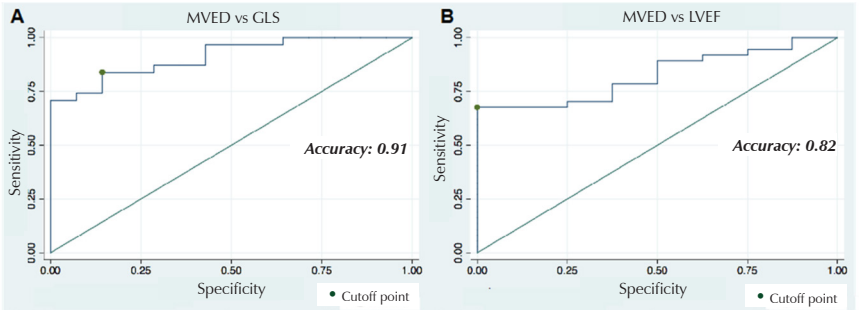

VMED: maximum velocity in early diastole LVEF: left ventricular ejection fraction.

Figure 7 – *(A) Receiver operating characteristic curve of global longitudinal strain and maximum atrioventricular junction displacement indicating the best cutoff point. (B) Maximum atrioventricular junction displacement and left ventricular ejection fraction performance.*

diastolic function by CMRI that, associated with its practical performance of both MD and MVED, can be considered a promising method for routine clinical use.

AVD presents with diastolic function disorders that precede evident LV systolic function changes that have important implications for morbidity and mortality before and after aortic valve replacement.[13–15] Several studies reported that LVEF is not affected early in groups of patients with AVD. A deteriorated ejection fraction in the clinical setting was considered a sign of severe and advanced AVD.[16–18] Several studies reported changed GLS and preserved LVEF in patients with AVD.[19–22]

GLS analysis after aortic valve replacement detected improved LV diastolic function measured by transmitral flow on ECHO. Similar studies also showed that GLS analysis after valve replacement indicated improved ventricular function.[23] GLS also showed less dependence on hemodynamic load conditions than LVEF, thus detecting more subtle changes in the underlying myocardial substrate.[24–26] Greater sensitivity for diagnosing diastolic dysfunction was observed after GLS evaluations in patients with AoS and AoI compared with conventional methods.[27] Analysis of the diagnostic performance of LLD parameters (MD and MVED) detects diastolic dysfunction in patients with AVD versus normal controls with a sensitivity similar to that of GLS. Diastolic function is rarely evaluated on CMRI because it depends on mitral, pulmonary vein, and myocardial flow velocity acquisition by cine-MRI with flow map (phase-contrast). Simple and practical MD and VDS measurements, especially the latter, represent a promising option for the diagnosis of diastolic dysfunction by CMRI that was validated in this study for patients with AVD.

VDS measurements and the VDS/MVED ratio also showed significant differences between pathological patients and normal controls, providing additional data in the assessment of diastolic dysfunction. However, the differences were smaller compared to those of MD and MVED, probably indicating less potential for their clinical application.

Limitations

This was a retrospective study with a relatively small number of patients. We also did not correlate LLD and GLS by ECHO; however, these parameters were validated by the CMRI myocardial tagging, a technique similar to the FTI used in this study as a reference, which mitigates this limitation. Finally, our new LLD method was validated only in patients with AVD; thus, future studies are needed to validate its use in patients with other diseases.

Conclusion

This study validated the LLD technique against GLS measured by FTI using CMRI. LLD parameters were obtained using only two linear measurements, which is possible with most image visualization software. Of the LLD parameters that assess systolic-diastolic function, MD showed better accuracy for assessing systolic function (normal values, less than -0.13), while MVED showed better accuracy for assessing diastolic function by CMRI (normal values, greater than 0.66). These parameters can improve the assessment of systolic-diastolic contractility in the clinical CMRI routine.

Acknowledgments

The authors thank the Zerbini Foundation for providing institutional support of this research project and Mrs. Lenira Cipriano for her support of the manuscript writing process.

Academic affiliation

This article represents scientific writing as a requirement to finish the internship project in scientific initiation of Rafael Almeida Fonseca, biomedicine student at Anhembi Morumbi University, held at the Cardiovascular Magnetic Resonance Sector of the Heart Institute (*Instituto do Coração* - InCor) of the School of Medicine, University of São Paulo (USP).

Ethical approval and consent information

This article is a sub-study of the project approved by the Research Ethics Committee of Hospital das Clínicas, School of Medicine, University of São Paulo (*Hospital das Clínicas da Faculdade de Medicina da Universidade de São Paulo* - HC FMUSP; no. 214,311). Due to the study's retrospective nature, the requirement for written informed consent was waived.

Authors' contribution

Fonseca RA, Ribeiro SM, Azevedo CF, Sampaio R, Tarasoutchi F, Rochitte CE contributed substantially to the study conception and design, data collection and analysis, and manuscript writing.

Conflict of interest

The authors have declared that they have no conflict of interest.

References

1. Del Castillo JM, Albuquerque ES, Silveira CA, Lamprea DP, Sena AD. Diastolicfunction assessment with doppler echocardiography and two-dimensional strain. Arq Bras Cardiol: Imagem cardiovasc 2017; 30(2): 46-53. DOI: 10.5935/2318-8219.20170012
2. Scatteia A, Baritussio A, Bucciarelli-Ducci C. Strain imaging using cardiac magnetic resonance. Heart Fail Rev. 2017;22(4):465-76. doi: https://doi.org/10.1007/s10741-017-9621-8
3. Claus P, Omar AM, Pedrizzetti G, Sengupta PP, Nagel E. Tissue Tracking Technology for Assessing Cardiac Mechanics: Principles, Normal Values, and Clinical Applications. JACC Cardiovasc Imaging. 2015;8(12):1444-60. doi: https://doi.org/10.1016/j.jcmg.2015.11.001
4. Pryds K, Larsen AH, Hansen MS, Grøndal AYK, Tougaard RS, Hansson NH, et al. Myocardial strain assessed by feature tracking cardiac magnetic resonance in patients with a variety of cardiovascular diseases - A comparison with echocardiography. Sci Rep. 2019;9(1):11296. doi: https://doi.org/10.1038/s41598-019-47775-4
5. Amundsen BH, Helle-Valle T, Edvardsen T, Torp H, Crosby J, Lyseggen E, et al. Noninvasive myocardial strain measurement by speckle tracking echocardiography: validation against sonomicrometry and tagged magnetic resonance imaging. J Am Coll Cardiol. 2006;47(4):789-93. doi: https://doi.org/10.1016/j.jacc.2005.10.040
6. Lopez-Candales A, Hernandez-Suarez DF. Strain Imaging Echocardiography: What Imaging Cardiologists Should Know. Curr Cardiol Rev. 2017;13(2):118-29. doi: https://doi.org/10.2174/1573403X12666161028122649
7. Mangion K, Burke NM, McComb C, Carrick D, Woodward R, Berry C. Feature-tracking myocardial strain in healthy adults- a magnetic resonance study at 3.0 tesla. Sci Rep. 2019;9(1):3239. doi: https://doi.org/10.1038/s41598-019-39807-w
8. Nagueh SF, Smiseth OA, Appleton CP, Byrd BF 3rd, Dokainish H, Edvardsen T, et al. Recommendations for the Evaluation of Left Ventricular Diastolic Function by Echocardiography: An Update from the American Society of Echocardiography and the European Association of Cardiovascular Imaging. J Am Soc Echocardiogr. 2016;29(4):277-314. doi: https://doi.org/10.1016/j.echo.2016.01.011
9. Saba SG, Chung S, Bhagavatula S, Donnino R, Srichai MB, Saric M, et al. A novel and practical cardiovascular magnetic resonance method to quantify mitral annular excursion and recoil applied to hypertrophic cardiomyopathy. J Cardiovasc Magn Reson. 2014;16(1):35. doi: https://doi.org/10.1186/1532-429X-16-35
10. Ribeiro SM, Azevedo Filho CF, Sampaio R, Tarasoutchi F, Grinberg M, Kalil-Filho R, et al. Longitudinal Shortening of the Left Ventricle by Cine-CMR for Assessment of Diastolic Function in Patients with Aortic Valve Disease. Arq Bras Cardiol. 2020;114(2):284-92. doi: https://doi.org/10.5935/abc.20190193
11. Simpson RM, Keegan J, Firmin DN. MR assessment of regional myocardial mechanics. J Magn Reson Imaging. 2013;37(3):576-99. doi: https://doi.org/10.1002/jmri.23756
12. Chen Q, Gan Y, Li ZY. Left ventricular diastolic dysfunction in type 2 diabetes patients: a novel 2D strain analysis based on cardiac magnetic resonance imaging. Comput Methods Biomech Biomed Engin. 2016;19(12):1330-8. doi: https://doi.org/10.1080/10255842.2016.1139093
13. Kumpuris AG, Quinones MA, Waggoner AD, Kanon DJ, Nelson JG, Miller RR. Importance of preoperative hypertrophy, wall stress and end-systolic dimension as echocardiographic predictors of normalization of left ventricular dilatation after valve replacement in chronic aortic insufficiency. Am J Cardiol. 1982;49(5):1091-100. doi: https://doi.org/10.1016/0002-9149(82)90032-7
14. Villari B, Hess OM, Kaufmann P, Krogmann ON, Grimm J, Krayenbuehl HP. Effect of aortic valve stenosis (pressure overload) and regurgitation (volume overload) on left ventricular systolic and diastolic function. Am J Cardiol. 1992;69(9):927-34. doi: https://doi.org/10.1016/0002-9149(92)90795-z
15. Bech-Hanssen O, Wallentin I, Houltz E, Beckman Suurküla M, Larsson S, Caidahl K. Gender differences in patients with severe aortic stenosis: impact on preoperative left ventricular geometry and function, as well as early postoperative morbidity and mortality. Eur J Cardiothorac Surg. 1999;15(1):24-30. doi: https://doi.org/10.1016/s1010-7940(98)00268-1
16. Lamb HJ, Beyerbacht HP, de Roos A, van der Laarse A, Vliegen HW, Leujes F, et al. Left ventricular remodeling early after aortic valve replacement: differential effects on diastolic function in aortic valve stenosis and aortic regurgitation. J Am Coll Cardiol. 2002;40(12):2182-8. doi: https://doi.org/10.1016/s0735-1097(02)02604-9
17. Faggiano P, Rusconi C, Ghizzoni G, Sabatini T. Left ventricular remodeling and function in adult aortic stenosis. Angiology. 1994;45(12):1033-8. doi: https://doi.org/10.1177/000331979404501206

18. Lund O, Flø C, Jensen FT, Emmertsen K, Nielsen TT, Rasmussen BS, et al. Left ventricular systolic and diastolic function in aortic stenosis. Prognostic value after valve replacement and underlying mechanisms. Eur Heart J. 1997;18(12):1977-87. doi: https://doi.org/10.1093/oxfordjournals.eurheartj.a015209

19. Vollema EM, Sugimoto T, Shen M, Tastet L, Ng AC, Abou R, et al. Association of Left Ventricular Global Longitudinal Strain With Asymptomatic Severe Aortic Stenosis: Natural Course and Prognostic Value. JAMA Cardiol. 2018;3(9):839-47. doi: https://doi.org/10.1001/jamacardio.2018.2288

20. Ng AC, Delgado V, Bertini M, Antoni ML, van Bommel RJ, van Rijnsoever EP, et al. Alterations in multidirectional myocardial functions in patients with aortic stenosis and preserved ejection fraction: a two-dimensional speckle tracking analysis. Eur Heart J. 2011;32(12):1542-50. doi: https://doi.org/10.1093/eurheartj/ehr084

21. Klaeboe LG, Haland TF, Leren IS, Ter Bekke RMA, Brekke PH, Røsjø H, et al. Prognostic Value of Left Ventricular Deformation Parameters in Patients with Severe Aortic Stenosis: A Pilot Study of the Usefulness of Strain Echocardiography. J Am Soc Echocardiogr. 2017;30(8):727-735.e1. doi: https://doi.org/10.1016/j.echo.2017.04.009.

22. Kusunose K, Goodman A, Parikh R, Barr T, Agarwal S, Popovic ZB, et al. Incremental prognostic value of left ventricular global longitudinal strain in patients with aortic stenosis and preserved ejection fraction. Circ Cardiovasc Imaging. 2014;7(6):938-45. doi: https://doi.org/10.1161/CIRCIMAGING.114.002041

23. Lamb HJ, Beyerbacht HP, de Roos A, van der Laarse A, Vliegen HW, Leujes F, Bax JJ, et al. Left ventricular remodeling early after aortic valve replacement: differential effects on diastolic function in aortic valve stenosis and aortic regurgitation. J Am Coll Cardiol. 2002;40(12):2182-8. doi: https://doi.org/10.1016/s0735-1097(02)02604-9

24. Erley J, Genovese D, Tapaskar N, Alvi N, Rashedi N, Besser SA, et al. Echocardiography and cardiovascular magnetic resonance based evaluation of myocardial strain and relationship with late gadolinium enhancement. J Cardiovasc Magn Reson. 2019;21(1):46. doi: https://doi.org/10.1186/s12968-019-0559-y

25. Knappe D, Pouleur AC, Shah AM, Cheng S, Uno H, Hall WJ, et al.; Multicenter Automatic Defibrillator Implantation Trial-Cardiac Resynchronization Therapy Investigators. Dyssynchrony, contractile function, and response to cardiac resynchronization therapy. Circ Heart Fail. 2011;4(4):433-40. doi: https://doi.org/10.1161/CIRCHEARTFAILURE.111.962902

26. Smedsrud MK, Pettersen E, Gjesdal O, Svennevig JL, Andersen K, Ihlen H, et al. Detection of left ventricular dysfunction by global longitudinal systolic strain in patients with chronic aortic regurgitation. J Am Soc Echocardiogr. 2011;24(11):1253-9. doi: https://doi.org/10.1016/j.echo.2011.08.003

27. Giritharan S, Cagampang F, Torrens C, Salhiyyah K, Duggan S, Ohri S. Aortic Stenosis Prognostication in Patients With Type 2 Diabetes: Protocol for Testing and Validation of a Biomarker-Derived Scoring System. JMIR Res Protoc. 2019;8(8):e13186. doi: https://doi.org/10.2196/13186